Cell PRESS
Open ACCESS

Cell Reports
Report

RYBP and Cbx7 Define Specific Biological Functions of Polycomb Complexes in Mouse Embryonic Stem Cells

Lluis Morey,[1,*] Luigi Aloia,[1] Luca Cozzuto,[1] Salvador Aznar Benitah,[1,2] and Luciano Di Croce[1,2,*]
[1]Centre for Genomic Regulation and UPF, Dr. Aiguader 88, 08003 Barcelona, Spain
[2]Institució Catalana de Recerca i Estudis Avançats, Pg. Lluis Companys 23, 08010 Barcelona, Spain
*Correspondence: lluis.morey@crg.eu (L.M.), luciano.dicroce@crg.eu (L.D.C.)
http://dx.doi.org/10.1016/j.celrep.2012.11.026

SUMMARY

The Polycomb repressive complex 1 (PRC1) is required for decisions of stem cell fate. In mouse embryonic stem cells (ESCs), two major variations of PRC1 complex, defined by the mutually exclusive presence of Cbx7 or RYBP, have been identified. Here, we show that although the genomic localization of the Cbx7- and RYBP-containing PRC1 complexes overlaps in certain genes, it can also be mutually exclusive. At the molecular level, Cbx7 is necessary for recruitment of Ring1B to chromatin, whereas RYBP enhances the PRC1 enzymatic activity. Genes occupied by RYBP show lower levels of Ring1B and H2AK119ub and are consequently more highly transcribed than those bound by Cbx7. At the functional level, we show that genes occupied by RYBP are primarily involved in the regulation of metabolism and cell-cycle progression, whereas those bound by Cbx7 predominantly control early-lineage commitment of ESCs. Altogether, our results indicate that different PRC1 subtypes establish a complex pattern of gene regulation that regulates common and nonoverlapping aspects of ESC pluripotency and differentiation.

INTRODUCTION

Polycomb group (PcG) repressor complexes (PRCs) are regulators of gene expression required for embryonic stem cell (ESC) fate decisions during development (Sauvageau and Sauvageau, 2010; Simon and Kingston, 2009). PRCs also affect the function of certain types of adult stem cells, and their misregulation contributes to tumorigenesis in several tissues (Piunti and Pasini, 2011). The two major complexes, PRC1 and PRC2, have been classified based on their composition as well as their enzymatic activity toward specific histone residues. The core of PRC2 is formed by the proteins Eed, Suz12, and Ezh1 and Ezh2 subunits. PRC2 deposits the histone H3 lysine 27 trimethyl repressive mark (H3K27me3) through the Ezh1/2 histone methyltransferase enzymes. Conversely, the canonical PRC1 consists of one of the Cbx proteins, polyhomeotic (PHC), PCGF, RYBP/YAF2, and a Ring1A/B E3 ligase subunit that monoubiquitinates histone H2A at lysine 119 (H2AK119ub) (Cao et al., 2002, 2005; Morey and Helin, 2010). Although both complexes are biochemically distinct, they can cooperatively establish epigenetic gene repression. In this sense, the canonical model of PRC-mediated gene silencing is based on the action of both complexes: PRC2 deposits the H3K27me3 mark, which creates a docking site for PRC1, recruiting it to chromatin through its direct recognition of the Cbx subunit. This two-step recruitment does not always occur; indeed, we and others have recently shown that PRC1 can also be recruited to chromatin in a PRC2-independent manner (Puschendorf et al., 2008; Richly et al., 2010; Schoeftner et al., 2006; Tavares et al., 2012).

The composition of PRC1 is highly complex. The protein families that constitute the core of PRC1 contain several members: Cbx (Cbx2, Cbx4, Cbx6, Cbx7, or Cbx8); Ring1A or Ring1B; PHC (PHC1, PHC2, or PHC3); PCGF (PCGF1, PCGF2, PCGF3, PCGF4, PCGF5, or PCGF6); and RYBP or YAF2. Each combination establishes the subtype of PRC1 complexes (Gao et al., 2012; Luis et al., 2012; Morey et al., 2012; O'Loghlen et al., 2012). For instance, mouse ESCs contain two main types of PRC1, which are defined by the mutually exclusive presence of Cbx7 or RYBP (Tavares et al., 2012). Cbx7 is the predominant PRC1-associated Cbx subunit in proliferating ESCs and requires the H3K27me3 mark to localize to chromatin and thereby silence the expression of lineage commitment genes. Once ESCs differentiate, other Cbx proteins, including Cbx2 and Cbx4, replace Cbx7 within PRC1 to mediate fate choices along the three germ layers (Morey et al., 2012). In contrast to Cbx7-PRC1, RYBP-PRC1 does not seem to require the H3K27me3 mark to bind to chromatin in ESCs (Luis et al., 2012; Tavares et al., 2012).

Here, we investigated the following questions about the PRC1 complexes that contain either Cbx7 or RYBP:

- What is the genome-wide localization of these two types of PCR1 complexes?
- Is the expression of specific sets of genes differentially regulated by both complexes?
- Do they exert common and/or unique biological functions?
- Do they show any interdependency for localizing to chromatin?

Our genome-wide studies indicate that RYBP-PRC1 and Cbx7-PRC1 complexes target a wide range of both overlapping and specific genes to exert their biological function in ESCs. Mechanistically, Cbx7 and RYBP do not depend on each other to bind to chromatin but do require Ring1A and Ring1B for their genomic localization. Nonetheless, even though depletion of either Cbx7 or RYBP reduced the level of H2AK119ub at target genes, only the knockdown of Cbx7 diminished the amount of Ring1B localized to chromatin. This suggests that RYBP is required to enhance the E3 ligase activity of Ring1B rather than its genomic binding. Surprisingly, genes bound by RYBP generally displayed lower levels of Ring1B and H2AK119ub than those containing Cbx7. Functional characterization indicates that RYBP target genes predominantly regulate cellular metabolism and the M phase of meiosis, whereas those bound by Cbx7 are strongly repressed and are associated with cell differentiation choices during early development.

RESULTS

RYBP-PRC1 and Cbx7-PRC1 Co-occupy Only a Subset of Target Genes in Mouse ESCs

Mouse ESCs contain at least two major types of PRC1 complexes, which are defined by the mutually exclusive presence of Cbx7 and RYBP (Tavares et al., 2012). Cbx7 is the predominant PRC1-associated Cbx subunit in ESCs, and virtually all of its target genes show Ring1B and PRC2 co-occupancy (Morey et al., 2012). We therefore sought to determine whether RYBP-PRC1 and Cbx7-PRC1 complexes are also mutually exclusive or whether they colocalize at the level of chromatin. To this end, we performed chromatin immunoprecipitation (ChIP) of RYBP followed by massive parallel sequencing (ChIP-seq) and compared these results to the genome-wide localization of Cbx7, Ring1B, and the PRC2 member Suz12 (Morey et al., 2012). We observed an overlap of RYBP peaks (3,918 in total) with 14%, 42%, and 37% of Cbx7, Ring1B, and Suz12 peaks, respectively (false discovery rate [FDR] = 1%; $p = 1 \times 10^{-5}$) (Figure 1A). Moreover, although more than 90% of Cbx7 peaks contained Ring1B and Suz12, 20% were also bound by RYBP (Figure 1A). Thus, whereas RYBP and Cbx7 display a high level of exclusive binding to chromatin, they also colocalize to a significant number of genomic regions. The extent of these overlaps did not significantly change when we analyzed putative target genes by focusing on an area spanning ±2.5 kb from the ChIP-seq peak summits. In this analysis, 50% of genes bound by RYBP contained Ring1B, and 31% (725 genes) overlapped with Cbx7 and PRC2 (Figures 1B and 1C). In contrast, and as previously published, virtually every gene occupied by Cbx7 contained Ring1B (Figure 1B). Overall, our ChIP-seq analysis allowed us to identify five types of genes according to the occupancy of PRC1 and PRC2: those with (1) Ring1B/Cbx7/RYBP and Suz12 (725 genes); (2) Ring1B/Cbx7/Suz12, but not RYBP (1,527 genes); (3) Ring1B/RYBP/Suz12, but not Cbx7 (861 genes); (4) only Ring1B and Suz12 (1,694 genes); or (5) RYBP but no Polycomb proteins (1,674) (Figure 1C).

Interestingly, the RYBP peak summits fell exactly at the transcription start sites (TSSs), whereas on average, the peak summits for Cbx7 are located approximately 0.5–1 kb downstream of the TSSs (Figure S1A). Sequential ChIP (re-ChIP) experiments of two RYBP and Cbx7 common target genes confirmed that the PRC1-RYBP and PRC1-Cbx7 complexes bind to the same loci (Figure S1B).

We next analyzed the intensity of the Ring1B and Suz12 signal at Cbx7 and RYBP peaks. Intriguingly, the level of Ring1B and Suz12 occupancy is on average higher at Cbx7 targets than at RYBP targets (Figure S1C). In other words, RYBP target genes contained less Ring1B than those bound by Cbx7-Ring1B (Figure S1D). Because PRC2 binds to CpG island-containing genes, and CpG islands are sufficient to recruit PRC2 (Ku et al., 2008; Mendenhall et al., 2010), we next asked whether the number of CpG islands was the underlying cause for the difference in PRC2 content and the amount of RYBP and Cbx7 at their target genes. Indeed, we found that 81% and 69% of total Cbx7 and RYBP peaks, respectively, contained at least one CpG island (Figure S1E). These differences were maintained when we focused on target genes; in this sense, whereas 98% of Ring1B/Cbx7/RYBP cotargets contained CpG islands, this percentage decreased to 80% in genes that have Ring1B and RYBP, but no Cbx7 (Figure S1E). Thus, genes bound by Cbx7-Ring1B contain on average a higher number of CpG islands than those bound by RYBP-Ring1B.

Next, we analyzed the binding profile and the peak intensity of the five different groups of genes reported in Figure 1C. This detailed analysis revealed that the binding of Ring1B and Suz12 gradually changed depending on the presence of Cbx7 and RYBP. Indeed, we observed that the binding of Ring1B/Suz12 was highest at genes cobound by RYBP and Cbx7 (compare Figure 1D with Figures 1E–1G), reduced at genes bound by Cbx7 but not RYBP, and even lower at genes occupied by RYBP but not Cbx7 (compare Figure 1E with Figure 1F). Genes without significant binding for Cbx7 or RYBP contained minimal amounts of Ring1B and Suz12 at their TSSs (Figure 1G). Additionally, we identified a cohort of genes that was only occupied by RYBP but not by any other Polycomb proteins, suggesting that RYBP functions at those genes independently of the PRC1 complex (Figure 1H) (Hisada et al., 2012). Thus, Cbx7 and RYBP occupancy correlates with that of Ring1B and Suz12. A reverse analysis further confirmed these observations. Indeed, the Ring1B/Suz12 average peak intensity was highest at genes co-occupied by Cbx7 and/or RYBP (Figure 1I). Notably, some of the genes that, based on the setting of our bioinformatic analysis, appeared not to be targeted by Cbx7 and/or RYBP showed very low amounts of Cbx7/RYBP when monitored by ChIP-qPCR (Figure S1F).

The Biological Significance of Different Levels of H2AK119ub at Ring1B/RYBP and Ring1B/Cbx7 Targets

We next determined whether the difference in the average amount of Ring1B between RYBP and Cbx7 targets was reflected by differences in the level of its enzymatic readout, which is the level of H2AK119ub at its target genes. We performed this analysis by focusing on (1) genes with Ring1B/Cbx7/RYBP and Suz12 (Figure 2A); (2) genes with Ring1B/RYBP/Suz12 but not Cbx7 (Figure 2B); and (3) genes with Ring1B/Cbx7/Suz12 but with either no RYBP (such as *Foxd2* and *GDNF*) or very low amounts of RYBP (such as *Pitx2*) (Figure 2C; see Experimental

A

Number of peaks	Overlapping	%
Cbx7: 2754	RYBP: 554	20.1
	Ring1B: 2536	92.1
	Suz12: 2538	92.1
Ring1B: 6982	Cbx7: 2463	35.2
	RYBP: 1660	23.7
	Suz12: 5721	82
RYBP: 3918	Cbx7: 578	14.7
	Ring1B: 1689	43.1
	Suz12: 1475	37.6
Suz12: 8054	Cbx7: 2521	31.3
	RYBP: 1447	18
	Ring1B: 5830	72.4

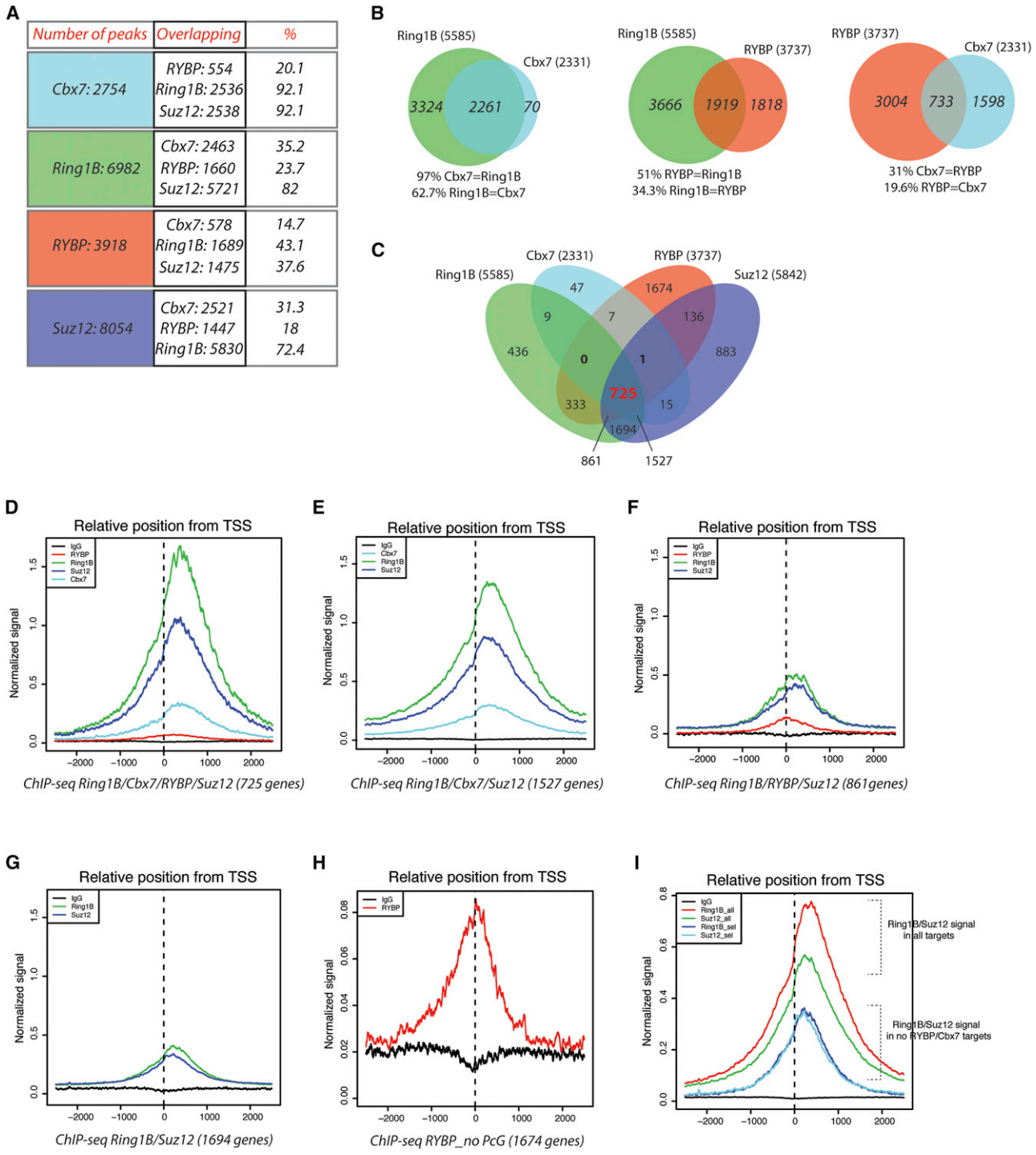

Figure 1. RYBP and Cbx7 Target Genes Are Not Mutually Exclusive in Mouse ESCs

(A) Peaks of Cbx7, Ring1B, RYBP, or Suz12, as identified by ChIP-seq in ESCs.

(B) Venn diagrams of Ring1B target genes that overlapped with Cbx7 or RYBP targets in ESCs.

(C) Venn diagrams of the overlap between target genes of Cbx7, Ring1B, RYBP, and Suz12.

(D–H) Normalized signal of the RYBP, Cbx7, Ring1B, Suz12, and IgG peaks, identified by ChIP-seq, relative to the TSS. The input reads were clustered in the different groups selected from (C) and described at the bottom of each graph.

(I) Normalized signal of the Ring1B, Suz12, and IgG peaks, identified by ChIP-seq, relative to the TSS. The input reads were clustered in two groups of Suz12 and Ring1B from all target genes and targets that do not have Cbx7 and RYBP.

Related to Figure S1.

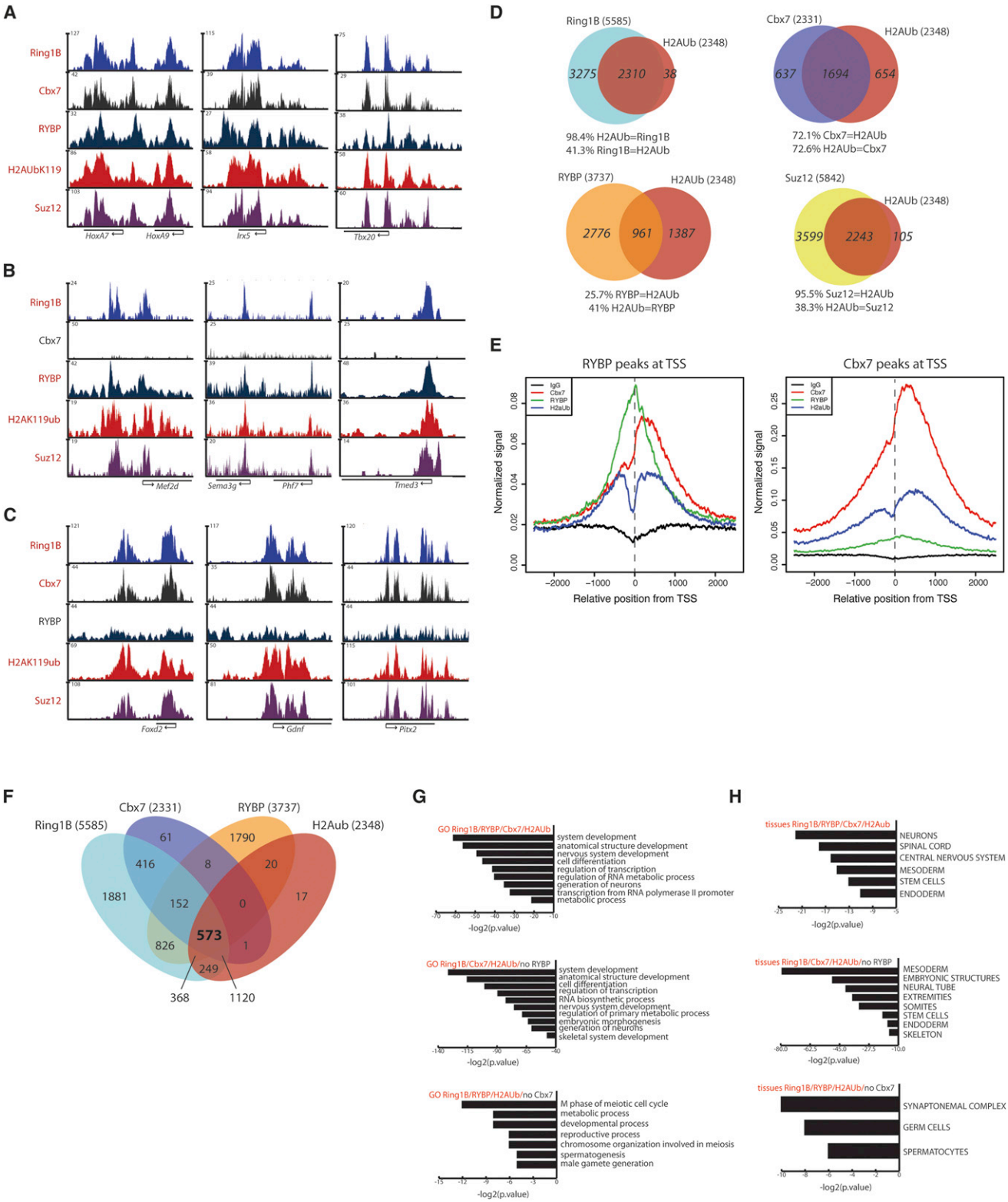

Figure 2. Cbx7 Target Genes Contain More H2AK119ub and Have Different Biological Functions than RYBP Target Genes

(A–C) UCSC screen shots of the profiles of the Ring1B, Cbx7, RYBP, H2AK119ub, and Suz12 ChIP-seq results for selected genes. The numbers at the top left of each graph represent the number of reads for each ChIP-seq profile of the given gene.

(D) Venn diagrams of H2AK119ub target genes that overlapped with Ring1B, Cbx7, RYBP, or Suz12 targets.

(legend continued on next page)

Procedures). Our results indicate that the vast majority of genes containing H2AK119ub are also occupied by Ring1B and Suz12 (Figures 2D and 2F). Interestingly, H2AK119ub was present in only 25.7% of RYBP target genes but in 72% of Cbx7 target genes (Figure 2D). Unexpectedly, the levels of H2AK119ub dropped at the RYBP peak summit at TSSs (Figure 2E), whereas the H2AK119ub profile perfectly correlated with high levels of Cbx7 (Figures 2E and S2A). Interestingly, four times more genes were co-occupied by Ring1B/Cbx7 and H2AK119ub (1,120 genes) than by Ring1B-RYPB and H2AK119ub (368 genes), whereas 573 genes contained Ring1B/RYBP/Cbx7/Suz12 and H2AK119ub (Figures 2F and S2B; Table S1). Together, these data support the presence of three major types of PRC1 target genes: a first set with Cbx7/Ring1B/H2AK119ub; a second that contains RYBP and lower levels of Ring1B/H2AK119ub (Figure 2E; note different y axis scale); and a third set cobound by RYBP/Cbx7/Ring1B and that also contains H2AK119ub.

We next asked whether these cohorts of genes represent different biological functions. Gene ontology (GO) analysis of biological function revealed that genes co-occupied by Ring1B/Cbx7/RYBP and H2AK119ub are involved in system development. Interestingly, genes containing RYBP/Ring1B/H2AK119ub, but not Cbx7, have a strong association with the M phase of the meiotic cycle and cellular metabolism (Figure 2G). Conversely, genes with Cbx7/Ring1B/H2AK119ub are involved in developmental processes and mesoderm specification, whereas those containing RYBP/Cbx7/Ring1B/H2AK119ub predominantly represent the ectodermal fate and, to a lesser extent, mesoderm and endoderm fates (Figures 2G and 2H).

The three sets of PRC1 target gene subtypes not only differed in their biological functions but also in the pathways they represented. In this sense, the KEGGS signaling pathway analysis revealed that Cbx7/RYBP/Ring1B/H2AK119ub target genes mainly repress Hedgehog and Wnt signaling, whereas those belonging to the RYBP/Ring1B/H2AK119ub set regulate Wnt and ErbB signaling genes, and those with Ring1B-Cbx7-H2AK119ub are involved in axon guidance and its main regulatory pathway of Hedgehog signaling (Table S2). Altogether, these results indicate that different combinations of PRC1 bound at chromatin establish a complex pattern of gene expression, each of which regulates a specific set of functions relevant to the biology of ESCs.

PRC1-RYBP Target Genes Are More Highly Expressed than PRC1-Cbx7 Targets

Re-ChIP experiments using Ring1B and active RNA-PolII antibodies have indicated that Ring1B and active RNA-PolII do not occupy the same allele, suggesting that PRC1 represses one allele, whereas the other is highly expressed (Brookes et al., 2012). To study the transcriptional status of the different PRC1-RYBP and PRC1-Cbx7 genes, we analyzed available ChIP-seq data (Brookes et al., 2012) of the elongation form of the RNA-PolII (RNA-PolII-S2p+) and compared it with our Ring1B, Cbx7, and RYBP ChIP-seq data sets. Interestingly, more than twice as many of total RYBP targets contained RNA-PolII-S2p as did Cbx7 targets (Figure S3A), whereas about 60% of Ring1B/RYBP and 37% of Ring1B/Cbx7 cotargets also had the elongated RNA-PolII (Figure 3A); importantly, this ratio was also maintained when H2AK119ub targets were included in the analysis (Figures S3B and S3C).

To further strengthen the proposal that Ring1B/RYBP targets are more highly expressed than Ring1B/Cbx7 targets, we analyzed the expression of these genes using our microarray and RNA-seq data from ESCs. Indeed, Ring1B/RYBP cotargets are more highly expressed on average than genes containing Ring1B/Cbx7 or Ring1B/Cbx7/RYBP (Figures 3B and 3C). Moreover, RYBP target genes that were not co-occupied by any Polycomb proteins were more highly expressed than the average expression of all genes (Figures 3C and S3D).

We then randomly selected four genes from each group of PRC1 target genes (i.e., those containing Cbx7/RYBP/Ring1B, Cbx7/Ring1B, or RYBP/Ring1B). In accordance with our previous observations (Figures 3A–3C), the four selected RYBP/Ring1B target genes were expressed to a significantly higher degree than those containing Cbx7/RYBP/Ring1B or Cbx7/Ring1B (Figure S3E). Interestingly, these genes were upregulated when Ring1B was depleted, and this upregulation was enhanced when both Ring1A and Ring1B were depleted (Figure 3D).

Recruitment of RYBP and Cbx7 to Chromatin

As mentioned above, purification of RYBP- and Cbx7-associated proteins in mouse ESCs revealed a mutually exclusive association to Ring1B-containing complexes. We have recently shown that Ring1B, Mel18, and Suz12 are significantly, but not completely, displaced from their target genes following Cbx7 depletion (Morey et al., 2012). We thus determined which factors are required for recruiting the different subtypes of PRC1 to chromatin. As shown in Figure 3E, Ring1B$^{-/-}$ ESCs had reduced occupancy of both Cbx7 and RYBP, and this effect was enhanced after double depletion of Ring1A/B. In contrast, deletion of Ring1A alone did not alter the binding of either Cbx7 or RYBP (Figures 3E and S3F; see also Morey et al., 2012).

Because our analysis identified more than 700 genes containing RYBP/Cbx7/Ring1B, we next asked whether depletion of Cbx7 affected the binding of RYBP to its target genes, and vice versa (Figure 4A). Interestingly, ChIP-qPCR of shared RYBP-Cbx7 target genes revealed that depletion of Cbx7 did not reduce RYBP occupancy at chromatin but in fact slightly increased it, even though the overall levels of Ring1B, Mel18, and H2AK119ub in chromatin were reduced (Figure 4B). Re-expression of a knockdown-resistant form of Cbx7 restored

(E) Normalized signal of all H2AK119ub, Ring1B, Cbx7, and IgG peaks that were identified by ChIP-seq, relative to the TSSs. The input reads were clustered into two groups: RYBP peaks and Cbx7 peaks.
(F) Venn diagrams of the overlap between target genes of Cbx7, Ring1B, RYBP, and H2AK119ub.
(G and H) GO analysis of biological functions and tissue-related genes of genes coregulated by PCR1 complexes containing Ring1B/RYBP/Cbx7, Ring1B/RYBP, Ring1B/Cbx7, or only RYBP. p Values are plotted in −log.
Related to Figure S2.

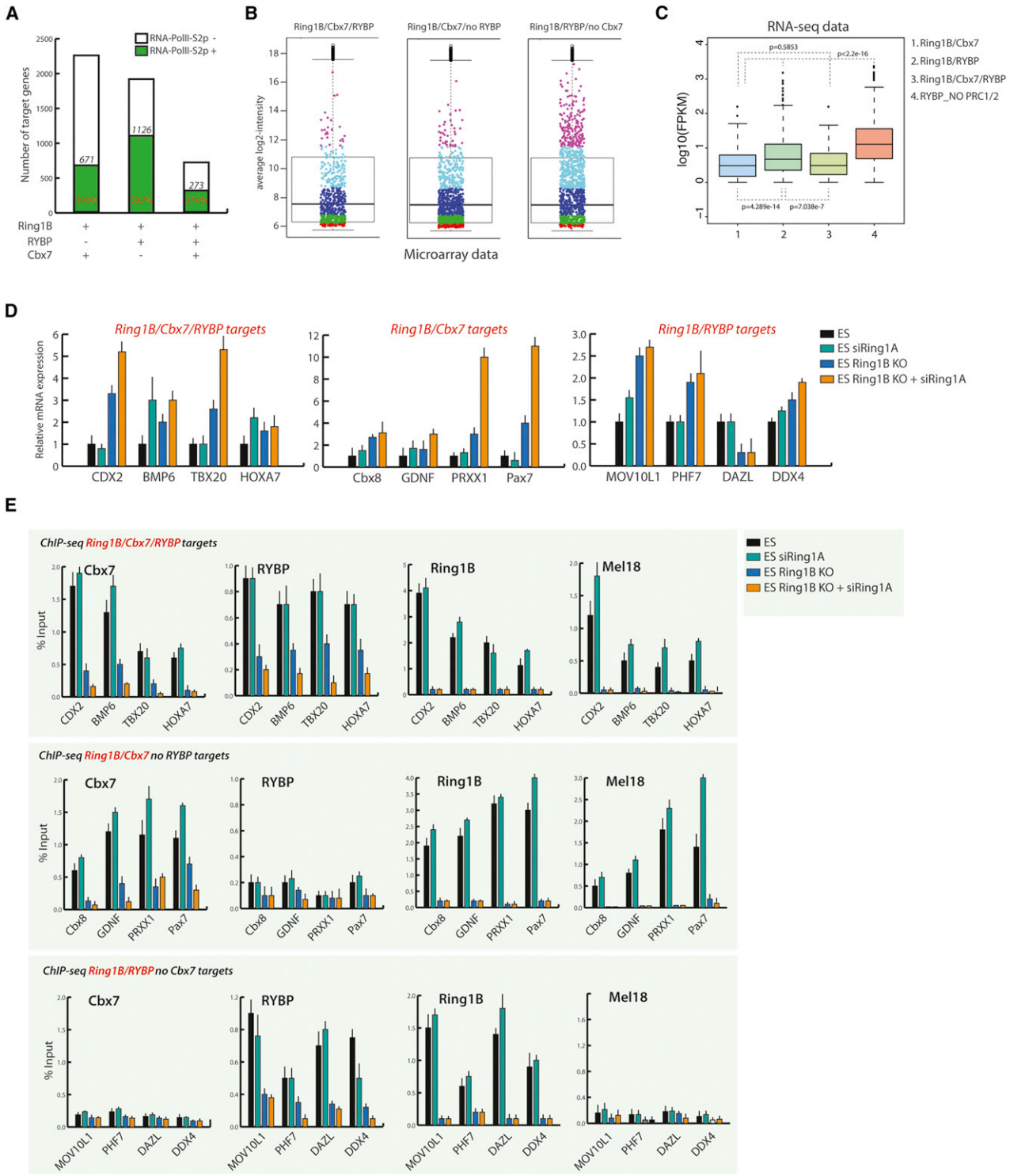

Figure 3. RYBP/Ring1B Target Genes Are More Likely to Be Expressed than Cbx7/Ring1B Targets

(A) Ring1B-associated genes with either RYBP and/or Cbx7 together with RNA-PolII-S2p.

(B) Gene expression analysis of Ring1B, RYBP, and Cbx7 target genes from microarray data in mouse ESCs. Expression levels were divided into three categories (see Experimental Procedures). The box plot represents the average gene expression for all the probes from the microarray.

(C) Gene expression analysis of Ring1B, RYBP, and Cbx7 target genes from RNA-seq data in mouse ESCs (Brookes et al., 2012). Box plots depict genes containing Ring1B/Cbx7/RYBP, Ring1B/Cbx7, Ring1B/RYBP, or RYBP with no PRC1/2. FPKM (fragments per kilobase of exon per million fragments mapped) values from RNA-seq data are shown.

(legend continued on next page)

the occupancy of chromatin factors to levels comparable to those observed in control cells (Figure 4B). On the other hand, ESCs depleted for RYBP showed reduced amounts of H2AK119ub, although the recruitment of the PRC1 subunits was not affected (Figure 4C). Although some residual RYBP protein was still present in RYBP-depleted cells, which could in part account for the lack of Ring1B displacement, our data are in agreement with Ring1B ChIP analysis performed in RYBP$^{-/-}$ ESCs (Hisada et al., 2012). Interestingly, we did not observe any compensation of RYBP or Cbx7 in ESCs depleted of Cbx7 or RYBP, respectively (Figures S4A and S4B). At the functional level, expression analysis of common Cbx7/RYBP target genes suggested that Cbx7 at those promoters plays an important role in maintaining gene repression (Figure 4D). The expression levels of RYBP targets (that are not Cbx7 targets) were further elevated upon depletion of RYBP, as previously reported in RYBP$^{-/-}$ ESCs (Figure 4D; Hisada et al., 2012). We next generated ESCs depleted of Cbx7 and RYBP (dKD-ESCs) (Figures S4C and S4D). Interestingly, dKD-ESCs expressed normal *Oct4* and *Nanog* mRNA and protein levels and did not display spontaneous differentiation (Figure S4E). We then asked whether the depletion of both Cbx7 and RYBP enhanced the derepression of genes containing both Cbx7-Ring1B and RYBP-PRC1 complexes. Intriguingly, *HOXA7* expression, which was not affected in cells depleted by either Cbx7 or RYBP alone, was 4-fold upregulated in dKD-ESCs. Moreover, *HOXA5* and *HOXD10* expression was strongly upregulated in dKD-ESCs, whereas their upregulation was more modest in Cbx7- or RYBP-depleted cells (Figure S4F). We conclude that both PRC1 complexes can functionally cooperate to regulate specific genes. Note that Ring1B binding was not completely displaced from chromatin in dKD-ESCs and that the H2AK119ub levels remained very similar to the levels found in Cbx7- or RYBP-depleted ESCs (Figures S4G and S4H).

Overall, these data suggest that Cbx7 plays an important role in Ring1B and Mel18 deposition at chromatin and that PRC1 binding does not depend on RYBP in proliferating ESCs. However, RYBP is necessary for the efficient enzymatic activity of Ring1B at target genes.

DISCUSSION

Recent data suggested that RYBP and Cbx form mutually exclusive PRC1 complexes, yet a comprehensive analysis of their genome-wide occupancy and a characterization of their molecular and biological function(s) in ESCs have not yet been reported. Here we demonstrate that (1) Cbx7 and RYBP occupy specific targets but also colocalize at a significant number of genomic regions; (2) the PRC1-Cbx7 complex largely overlaps with H2AK119ub; (3) expression of Ring1B/RYBP target genes is on average significantly higher than that of Ring1B/Cbx7 targets; and (4) binding of other PRC1 components, such as Mel18 and Ring1B, to chromatin mainly relies on the presence of Cbx7, whereas the efficient enzymatic activity of PRC1 requires RYBP.

We have identified more than 700 genes targeted by PRC1-RYBP, PRC1-Cbx7, and PRC2. The profile analysis of Cbx7 and RYBP occupancy indicates that, whereas Cbx7 peaks were at TSSs, RYBP peaks were one to two nucleosomes upstream. This suggests that different complexes might exert different functions with respect to promoter regulation and might possess different recruiting mechanisms. This hypothesis is further supported by the finding that 861 of the PRC1-RYBP target genes also are bound by Suz12, whereas 331 have no Suz12, indicating a higher level of complexity for Polycomb recruitment than anticipated. The exact manner in which PRC1-RYBP is recruited to chromatin is still unknown. Protein domain analysis predicts that RYBP only possesses a single Zn finger-RanBP2 domain. So far, this family of zinc finger domains has only been implicated in protein-protein interactions, yet previous data suggest that RYBP binds directly to DNA (Neira et al., 2009). However, PRC1-RYBP could also be recruited to DNA by other modes, such as through its direct interactions with transcription factors and/or noncoding RNAs. Finally, Mel18 and Cbx7 binding was found to be very low at RYBP-Ring1B target genes, suggesting that other highly expressed PCGF proteins, such as NSPC1 and MBLR, might associate with RYBP-PRC1 complexes. In line with this, Tavares and colleagues have shown that Mel18, NSP1, and MBLR are strongly associated with RYBP in ESCs (Tavares et al., 2012). Thus, we hypothesize that a further layer of PRC1 complexity might exist in ESCs: different RYBP-Ring1B complexes containing specific PCGF proteins could modulate enzymatic activities that have specific biological functions. The presence of specific PCGF proteins within the RYBP-Ring1B complex could modulate its enzymatic activities and specify different biological functions.

The enzymatic activities of PRC1-RYBP and PRC1-Cbx7 complexes are still under debate. In vitro assays using recombinant Ring1B/Mel18 complexes containing either RYBP or Cbx7 are both able to efficiently monoubiquitinate H2A (Tavares et al., 2012), although recombinant PRC1-RYBP seems more enzymatically active than PRC1 containing Cbx2 or Cbx8 (Gao et al., 2012). Interestingly, nucleosomal arrays incubated with recombinant PRC1 containing either RYBP or Cbx2 revealed that the complex with RYBP compacted chromatin more efficiently than the complex with Cbx2 (Gao et al., 2012). Our data indicate that Cbx7 target genes are associated with higher levels of H2AK119ub as compared to RYBP targets. This might suggest that, in vivo, Cbx7 increases PRC1 activity to a greater extent than RYBP or Cbx2; alternatively, PRC1-RYBP complexes could catalyze the deposition of the H2AK119ub mark and then be replaced by PRC1-Cbx7 complexes.

(D) qRT-PCR of selected genes from three gene categories in wild-type (WT) ESCs, siRing1A ESCs, Ring1B knockout (KO) ESCs, and Ring1A/B-depleted mouse ESCs.

(E) Cbx7 and RYBP binding is dependent on Ring1B/A. qPCR of the indicated gene promoters, at the bottom of the panels, after ChIP experiments in control, Ring1A-depleted, Ring1B KO, or Ring1B KO/siRing1A ESCs, performed with the antibodies indicated in the graphs. Results are presented as a percentage of input material. All ChIP experiments represent the average of three independent experiments.

Related to Figure S3.

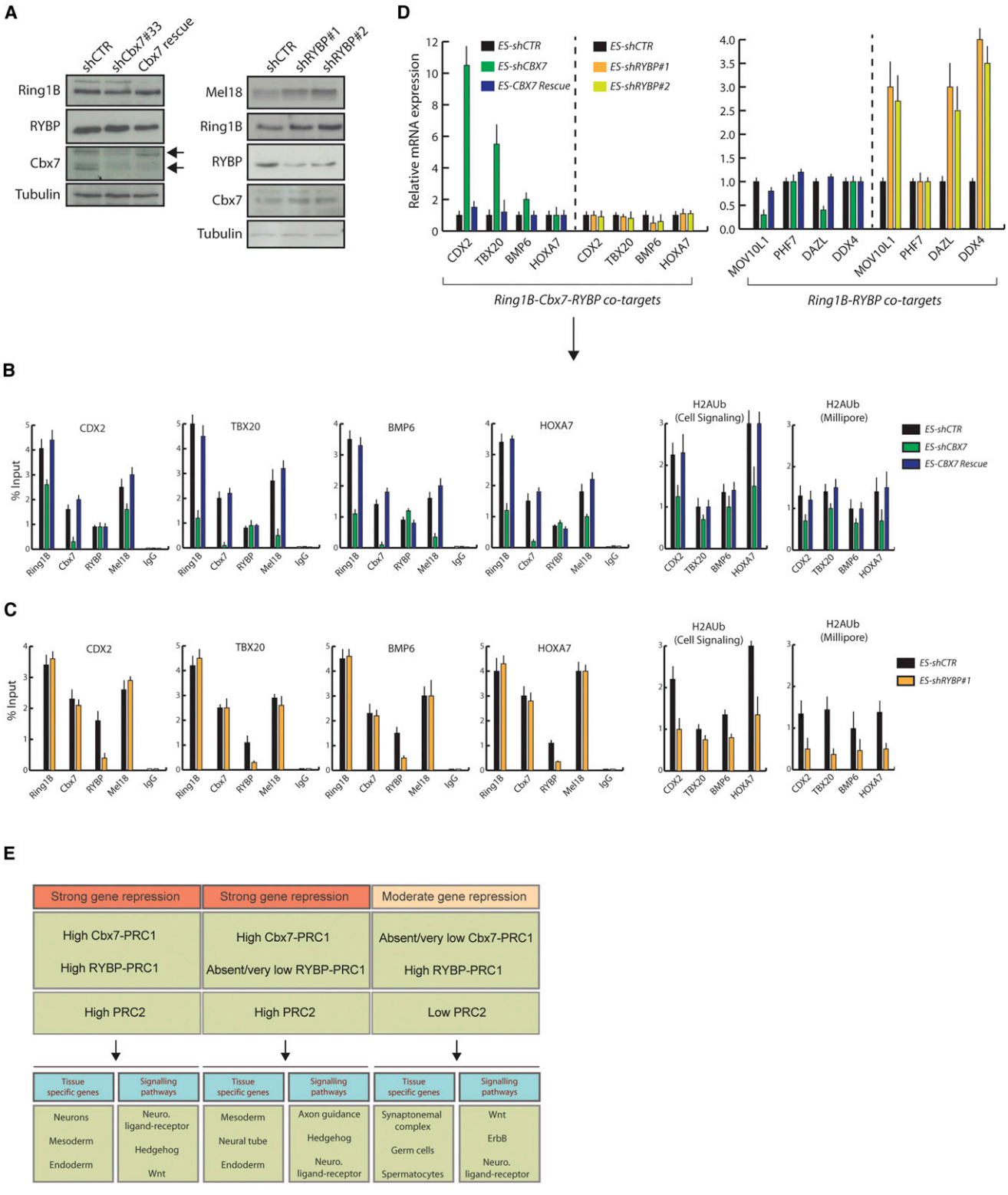

Figure 4. Interdependency of RYBP and Cbx7 Recruitment to Chromatin

(A) Western blot analysis of different PRC1 subunits from total cell extracts of shCTR, shCbx7, and shRYBP mouse ESCs. Tubulin was used as a loading control.

(B) ChIP-qPCR of selected Cbx7 and RYBP target genes in shCTR, shCbx7-depleted, or 3× Flag-Cbx7 rescue ESCs. The IgG antibody was used as a negative control. Results are presented as percentage of input material immunoprecipitated and represent an average of three independent experiments.

(legend continued on next page)

A recent report has shown that a set of PRC1 target genes, termed *PRCa*, is highly expressed (Brookes et al., 2012). Our analysis indicates that RYBP/Ring1B target genes are more highly expressed than those containing Cbx7 alone or those co-occupied by Cbx7 and RYBP, suggesting that the PRC1 complex bound to *PRCa* genes most likely contains RYBP rather than Cbx7. RYBP/Ring1B targets are associated with metabolic pathways and more involved in the M phase of meiosis than in developmental pathways. Therefore, the differential composition of the PRC1 complex (e.g., containing either Cbx7 or RYBP) could determine which category of genes it regulates.

In mouse ESCs, Cbx7 is necessary for recruiting Ring1B, but not RYBP, and for maintaining genes in a silenced state. The observation that RYBP binding to chromatin is slightly increased after Cbx7 depletion might indicate that, under these conditions, compensatory mechanisms are activated to counteract the lack of Cbx7. Interestingly, upon RYBP depletion, none of the PRC1 subunits was displaced from chromatin, yet the levels of H2AK119ub were slightly reduced. This indicates that the PRC1-Cbx7 complex is recruited to chromatin independently of RYBP but that PRC1 enzymatic activity requires RYBP to efficiently ubiquitinate histone H2A in the nucleus.

EXPERIMENTAL PROCEDURES

ESC Culture and Generation of Stable Knockdown ESCs

E14Tg2A ESCs were cultured feeder free in plates coated with 0.1% of gelatin as described previously. To produce lentiviruses containing shRNA, 293T cells (2×10^6) were transfected with 7 μg of pLKO-shRNA (Sigma-Aldrich), 5 μg of pCMV-VSV-G, and 6 μg of pCMVDR-8.91 plasmids. After 72 hr, ESCs were infected overnight by reverse infection with the virus-containing media filtered with LIF and polybrene (1 μg/ml). shCbx7 ESCs were selected 24 hr after infection with 2 μg/ml of puromycin (Sigma-Aldrich) and shRYBP ESC with 250 μg/ml of hygromycin. To generate stable dKD-ESCs, we infected RYBP knockdown ESCs with lentiviruses containing shRNA-Cbx7. dKD-ESCs were cultured under 2 μg/ml of puromycin and 250 μg/ml of hygromycin. The shRNA sequences are shown in Table S3.

ChIP and Re-ChIP Assays

ChIP was performed as described previously (Morey et al., 2012), with the following modifications. Due to the high background of the antibodies against RYBP (Millipore) and H2AK119ub (Cell Signaling), we modified the ChIP experiments as follows: for RYBP, 2 μl of antibody was incubated with 500 μg of protein for 2 hr, and for H2AK119ub, 1 μl of antibody (Cell Signaling) was incubated with 100 μg of protein for 2 hr. Immunocomplexes were recovered with 30 μl of protein A bead slurry saturated with salmon sperm, washed three times with low-salt buffer and two times with high-salt buffer. Primers and antibodies used are listed in Table S3. For re-ChIP assays, immunoprecipitated DNA was eluted after the last ChIP wash with 50 μl of 10 mM DTT for 30 min at 37°C and diluted 10× with ChIP buffer; 5 μg of antibody was then incubated with this overnight at 4°C with rotation.

ChIP-Seq Data Analyses

The millions of reads produced by ChIP-seq of RYBP, Cbx7, Ring1B, Suz12, and H2AK119Ub were aligned with the mouse genome (version NCBIM37) using the Bowtie (Langmead et al., 2009) tool version 0.12.7; two mismatches were allowed within the seed alignment. Sequence tags were aligned to the genome and then subsequently analyzed by MACS software version 1.4.1 (Zhang et al., 2008) to detect genomic regions enriched for multiple overlapping DNA fragments (peaks) that we considered to be putative binding sites. MACS estimated the FDR by comparing the peaks obtained from the samples with those from the control samples, using the same p value cutoff (1×10^{-5}). Peaks with a FDR lower than 5% from Cbx7, Ring1B, Suz12, and H2AK119ub, and lower than 1% from RYBP, were combined to detect chromosomal regions for further analyses. Genes with a peak within the gene body, or within 2.5 kb from the TSS, were considered to be target genes. An area of 5 kb surrounding each TSS that was associated to one or more ChIP-seq (RYBP, Ring1B, Cbx7, Suz12, or H2AK119ub) was used to calculate the ChIP-seq profile and the whole ChIP-seq coverage. ChIP-seq profiles around the TSSs were generated for each IP by calculating the average coverage in each position normalized for the total number of mapped reads with the BED tools package (Quinlan and Hall, 2010).

ACCESSION NUMBERS

Sequencing data have been deposited into the NCBI Gene Expression Omnibus database under accession number GSE42466.

SUPPLEMENTAL INFORMATION

Supplemental Information includes four figures and three tables and can be found with this article online at http://dx.doi.org/10.1016/j.celrep.2012.11.026.

LICENSING INFORMATION

ACKNOWLEDGMENTS

We are indebted to V.A. Raker for help in preparing the manuscript, to members of the L.D.C. laboratory for discussions, and to the CRG Genomic Unit. This work was supported by grants from the Spanish "Ministerio de Educación y Ciencia" (BFU2010-18692), from AGAUR, and from by European Commission's 7th Framework Program 4DCellFate grant number 277899 to L.D.C.; L.M. was supported by a postdoctoral CRG-Novartis fellowship.

Received: August 3, 2012
Revised: November 5, 2012
Accepted: November 28, 2012
Published: December 27, 2012

REFERENCES

Brookes, E., de Santiago, I., Hebenstreit, D., Morris, K.J., Carroll, T., Xie, S.Q., Stock, J.K., Heidemann, M., Eick, D., Nozaki, N., et al. (2012). Polycomb associates genome-wide with a specific RNA polymerase II variant, and regulates metabolic genes in ESCs. Cell Stem Cell *10*, 157–170.

Cao, R., Wang, L., Wang, H., Xia, L., Erdjument-Bromage, H., Tempst, P., Jones, R.S., and Zhang, Y. (2002). Role of histone H3 lysine 27 methylation in Polycomb-group silencing. Science *298*, 1039–1043.

(C) ChIP-qPCR of selected Cbx7 and RYBP target genes in shCTR- or shRYBP-depleted ESCs. The IgG antibody was used as a negative control. Results are presented as percentage of input material immunoprecipitated and represent an average of three independent experiments.
(D) qRT-PCR of Cbx7 and RYBP target genes. Expression was normalized to the housekeeping gene RPO. Data represent the average of three independent experiments.
(E) Model depicting three types of PRC1 target genes identified in ESCs, with specific biological functions.
Related to Figure S4.

Cao, R., Tsukada, Y., and Zhang, Y. (2005). Role of Bmi-1 and Ring1A in H2A ubiquitylation and Hox gene silencing. Mol. Cell *20*, 845–854.

Gao, Z., Zhang, J., Bonasio, R., Strino, F., Sawai, A., Parisi, F., Kluger, Y., and Reinberg, D. (2012). PCGF homologs, CBX proteins, and RYBP define functionally distinct PRC1 family complexes. Mol. Cell *45*, 344–356.

Hisada, K., Sánchez, C., Endo, T.A., Endoh, M., Román-Trufero, M., Sharif, J., Koseki, H., and Vidal, M. (2012). RYBP represses endogenous retroviruses and preimplantation- and germ line-specific genes in mouse embryonic stem cells. Mol. Cell. Biol. *32*, 1139–1149.

Ku, M., Koche, R.P., Rheinbay, E., Mendenhall, E.M., Endoh, M., Mikkelsen, T.S., Presser, A., Nusbaum, C., Xie, X., Chi, A.S., et al. (2008). Genomewide analysis of PRC1 and PRC2 occupancy identifies two classes of bivalent domains. PLoS Genet. *4*, e1000242.

Langmead, B., Trapnell, C., Pop, M., and Salzberg, S.L. (2009). Ultrafast and memory-efficient alignment of short DNA sequences to the human genome. Genome Biol. *10*, R25.

Luis, N.M., Morey, L., Di Croce, L., and Benitah, S.A. (2012). Polycomb in stem cells: PRC1 branches out. Cell Stem Cell *11*, 16–21.

Mendenhall, E.M., Koche, R.P., Truong, T., Zhou, V.W., Issac, B., Chi, A.S., Ku, M., and Bernstein, B.E. (2010). GC-rich sequence elements recruit PRC2 in mammalian ES cells. PLoS Genet. *6*, e1001244.

Morey, L., and Helin, K. (2010). Polycomb group protein-mediated repression of transcription. Trends Biochem. Sci. *35*, 323–332.

Morey, L., Pascual, G., Cozzuto, L., Roma, G., Wutz, A., Benitah, S.A., and Di Croce, L. (2012). Nonoverlapping functions of the Polycomb group Cbx family of proteins in embryonic stem cells. Cell Stem Cell *10*, 47–62.

Neira, J.L., Román-Trufero, M., Contreras, L.M., Prieto, J., Singh, G., Barrera, F.N., Renart, M.L., and Vidal, M. (2009). The transcriptional repressor RYBP is a natively unfolded protein which folds upon binding to DNA. Biochemistry *48*, 1348–1360.

O'Loghlen, A., Muñoz-Cabello, A.M., Gaspar-Maia, A., Wu, H.A., Banito, A., Kunowska, N., Racek, T., Pemberton, H.N., Beolchi, P., Lavial, F., et al. (2012). MicroRNA regulation of Cbx7 mediates a switch of Polycomb orthologs during ESC differentiation. Cell Stem Cell *10*, 33–46.

Piunti, A., and Pasini, D. (2011). Epigenetic factors in cancer development: polycomb group proteins. Future Oncol. *7*, 57–75.

Puschendorf, M., Terranova, R., Boutsma, E., Mao, X., Isono, K., Brykczynska, U., Kolb, C., Otte, A.P., Koseki, H., Orkin, S.H., et al. (2008). PRC1 and Suv39h specify parental asymmetry at constitutive heterochromatin in early mouse embryos. Nat. Genet. *40*, 411–420.

Quinlan, A.R., and Hall, I.M. (2010). BEDTools: a flexible suite of utilities for comparing genomic features. Bioinformatics *26*, 841–842.

Richly, H., Rocha-Viegas, L., Ribeiro, J.D., Demajo, S., Gundem, G., Lopez-Bigas, N., Nakagawa, T., Rospert, S., Ito, T., and Di Croce, L. (2010). Transcriptional activation of polycomb-repressed genes by ZRF1. Nature *468*, 1124–1128.

Sauvageau, M., and Sauvageau, G. (2010). Polycomb group proteins: multi-faceted regulators of somatic stem cells and cancer. Cell Stem Cell *7*, 299–313.

Schoeftner, S., Sengupta, A.K., Kubicek, S., Mechtler, K., Spahn, L., Koseki, H., Jenuwein, T., and Wutz, A. (2006). Recruitment of PRC1 function at the initiation of X inactivation independent of PRC2 and silencing. EMBO J. *25*, 3110–3122.

Simon, J.A., and Kingston, R.E. (2009). Mechanisms of polycomb gene silencing: knowns and unknowns. Nat. Rev. Mol. Cell Biol. *10*, 697–708.

Tavares, L., Dimitrova, E., Oxley, D., Webster, J., Poot, R., Demmers, J., Bezstarosti, K., Taylor, S., Ura, H., Koide, H., et al. (2012). RYBP-PRC1 complexes mediate H2A ubiquitylation at polycomb target sites independently of PRC2 and H3K27me3. Cell *148*, 664–678.

Zhang, Y., Liu, T., Meyer, C.A., Eeckhoute, J., Johnson, D.S., Bernstein, B.E., Nusbaum, C., Myers, R.M., Brown, M., Li, W., and Liu, X.S. (2008). Model-based analysis of ChIP-Seq (MACS). Genome Biol. *9*, R137.